Iranian Polymer Journal (2022) 31:1523–1535
https://doi.org/10.1007/s13726-022-01099-9

ORIGINAL RESEARCH

A mechanochemical approach for synthesizing almond shell nanoparticles and their potential application on the enhancement of polylactic acid film properties

Melinda Shali George Edward[1] · Antony Catherine Flora Louis[1] · Harini Srinivasan[1] · Sivakumar Venkatachalam[1]

Received: 3 February 2022 / Accepted: 26 July 2022 / Published online: 21 September 2022

Abstract
The utilization of biopolymers as a packaging material has received enormous attention, owing to the arising pressure on global warming and environmental pollution. Polylactic acid (PLA) is identified as a promising biopolymer with good processability amidst other biopolymers. However, due to its poor barrier property and brittle nature, its use is limited. To alleviate the properties of polymer composites, plasticization and reinforcement with nanoparticles are carried out in this study. Nanoparticles derived from naturals resources (almond shell wastes) are utilized for the present research due to the ecological concerns associated toward the usage of synthetic nanoparticles. Almond shell nanoparticles with an average particle size of 197 nm were prepared by ball milling and then ultrasonication. The influence of plasticizers, such as glycerol, sorbitol, polyethylene glycol, clove oil and polycaprolactone on the properties of biodegradable PLA films was investigated. The results revealed that PLA films blended with 10% (by w/w) naturally derived clove oil improved the elongation by 377.19% and the tensile strength up to 19.75 MPa. The PLA composite films with varied proportions of almond shell waste nanoparticles (0.25–1.0% by wt) were developed. At optimum loading, the tensile strength of PLA/0.75% (by wt) nanoparticle film increased to 25.09 MPa, and its water vapor permeability was reduced to 0.25×10^{-10} gPa^{-1} s^{-1} m^{-1} with the addition of 1% filler. The PLA films incorporated with nanoparticles displayed low transparency, increased water solubility and biodegradability compared to a neat PLA film. The results obtained demonstrated that the PLA developed, using almond shell wastes, is a better alternative to synthetic plastics in the packaging industries.

✉ Sivakumar Venkatachalam
drvsivakumar@yahoo.com

[1] Food Process Engineering Laboratory, Department of Chemical Engineering, AC Tech, Anna University, Chennai 600025, India

Graphical abstract

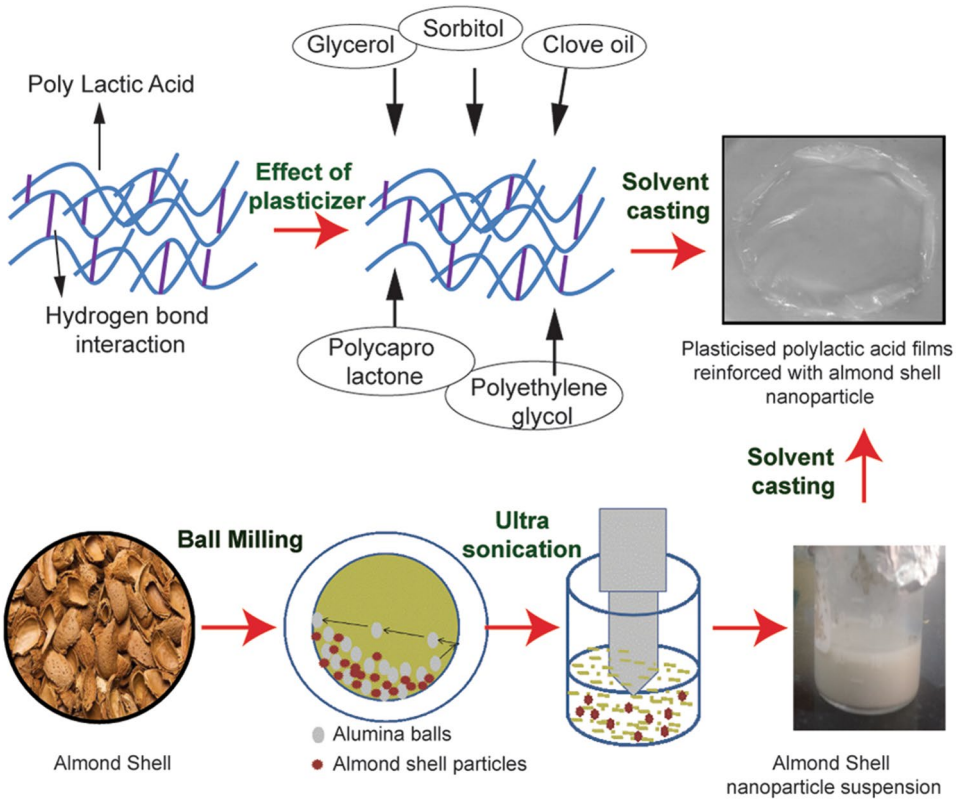

Keywords Polylactic acid · Plasticizer · Clove oil · Almond shell · Nanoparticle

Introduction

Polymers for food packaging applications have come across several evolutionary periods with the hope of developing packaging materials that have good properties and ecofriendly characteristics [1]. Traditional synthetic polymers were considered as ideal materials for food packaging applications; however, they have been causing serious damage to the environment in terms of exhaustion of fossil fuels, pollution and release of greenhouse gases [2, 3]. As much as 45% of these synthetic plastics are used in disposable food packaging that leads to the accumulation of municipal solid waste [2]. In this regard, a significant research has been oriented toward improving the properties of biopolymers to replace synthetic food packaging materials.

In an effort to develop a sustainable polymer that can possibly reduce the dependency on synthetic plastic, a number of ecofriendly biopolymers has come into play [4–7]. Polylactic acid (PLA) is one such thermoplastic biopolymer synthesized from lactic acid that has innate advantages, comprising of excellent mechanical properties, environment friendly nature, abundant availability, transparency, biocompatibility, resistance to ultraviolet rays, hydrophobicity and processability at a reasonable cost, making it an appropriate aspirant for replacement of fossil fuel-based polymers [8]. It is also recyclable, compostable and globally safe as it is free of greenhouse effect and it is approved by Food and Drug Administration, United States [9]. Despite the promising features of PLA, its application is limited due to poor barrier properties, low impact strength and brittleness of its films [10–12]. The most viable approach to improve the processability of PLA is by either copolymerization, grafting with other polymers, and addition of biofillers or by inclusion of plasticizers [13]. Among which plasticization and addition of biofillers have been shown to be simple and cost-effective methods to improve the flexibility and durability of PLA materials [14]. Plasticizers are widespread additives that are used to reduce the viscosity of the materials, thereby increasing the mobility between the molecules and increasing their workability [15]. Addition of plasticizer in PLA reduces the free volume in the polymer matrix and increases the flexibility of films. However, this strongly depends on the compatibility of the plasticizer and the polymer matrix. But the addition of plasticizer

consequently decreases the tensile strength and modulus of the films. Therefore, to balance the elongation and tensile strength of the films, a synergistic effect is required. One such possible strategy to achieve both these aspects is to prepare a plasticized PLA film reinforced with, a nanoparticle. Recent studies prove that the properties of pure PLA can be varied with the help of a different type of natural or biofillers, thereby designing a new class of materials called "biobased composites" [16]. As a result, currently, the use of natural biofillers over synthetic fillers has gained interest among researchers due to ecological concerns. Currently, researchers have been using biofillers obtained from natural fibers in polymeric matrices to improve their properties for producing biodegradable, low cost and ecofriendly composites [17, 18]. The dispersion of these nanofillers in polymeric matrices has proved to improve the mechanical, electrical, thermal and moisture resistance properties of the polymer [19].

Recent advances in nanotechnology have attracted the search for green and energy-efficient processing routes for synthesizing nanomaterials. Conventional acid hydrolysis, although promising, has drawbacks such as complexity of the process and low production yield, making it impractical for large-scale production. Therefore, fabrication of a new strategy is required. As per the 2016 statistics, around 3.21 million tons of almonds were reported to be produced globally [20]. However, the remaining parts of the almond fruit, such as the middle shell, almond hull and seed coat are considered agricultural wastes. Almond shells are regarded as a renewable lignocellulosic material. It is composed of cellulose of $38.47 \pm 0.39\%$ (by wt), hemicellulose of $28.82 \pm 0.25\%$ (by wt), and lignin of $29.54 \pm 0.11\%$ (by wt), respectively [21]. These shells are usually either dumped or incinerated, causing environmental pollution [22]. Therefore, to prevent these, various research works have been carried out using these shells [23–26]. With the growing demand to develop ecofriendly composites to reduce environmental issues, these almond shells can be used as biofiller in the polymer matrix. Few researchers have utilized these almond shell biofillers for use in commodity plastics like epoxy [27], polyethene [28], and polypropylene [29]. This research is focused on utilizing the biofiller derived from almond shell wastes on biopolymer PLA to replace the use of conventional plastics.

In this context, to synergistically increase the tensile and elongation property of the PLA film, a study has been attempted on plasticization and addition of nanoparticle in PLA films. A novel strategy is developed to prepare nanoparticles from almond shell waste through a mechanochemical approach. This study attempts to combine ball milling with ultrasonication for producing nanomaterials without minimizing the product yield at a reduced cost. Size reduction is achieved in ball milling through the application of kinetic energy to the material wherein materials are fractured to break their chemical bonds and produce new surfaces without minimizing the product yield. Therefore, this mechanochemical process promises to result in unique nanostructures with higher yield, while their potential as nanofillers in PLA film.

Experimental

Materials

Almond shells were collected from local vendors (Chennai, India). Polylactic acid (PLA) in pellet form with content of 94% *L*-lactic acid and 6% *D*-lactic acid was purchased from Natur-Tec, USA. The purchased film grade PLA was of specific gravity 1.3–1.4 g/cm^3 with a melting point of 110–120 ºC. Polyethylene glycol (PEG), glycerol (anhydrous extra pure AR, 99.5%), sorbitol (monostearate extra pure), clove oil (extra pure AR, 99.8%), polycaprolactone (extrapure AR, 99.8%), Tween80, sulphuric acid, and calcium chloride were supplied by Sigma-Aldrich (Bangalore, India). Dichloromethane (extra pure AR, 99.5%) was procured from Fischer Scientific.

Effect of plasticizer incorporation on PLA-based film

PLA pellet was added to dichloromethane (DCM) in a solid/liquid ratio of 1:50 and continuously stirred in a magnetic stirrer for 1 h. Tween80 (10%) was added as surfactant and stirring was continued. Plasticizer [glycerol, sorbitol, clove oil, polyethylene glycol (PEG) and polycaprolactone (PCL)] at various concentrations (2.5–15% w/w) were added to the film solution and stirred for 4 h. The solution was cast on a glass plate and was dried overnight at ambient conditions [30]. The films were then conditioned at 25 °C at 50% RH for 2 days prior to analysis. The plasticizer effect on the improvement of mechanical, optical, barrier, thermal and biodegradability was studied.

Preparation of almond shell nanoparticles (ANP)

The powdered almond shell was ball-milled using a planetary ball milling machine with seven alumina balls of the same diameter (~ 15 mm). Two grams of the sample and 20 mL of 1% sulphuric acid were added to the ceramic bowl along with the alumina balls. The mixture was milled at 300 rpm for 3 h. The obtained slurry was diluted with distilled water till it reached neutral pH and was then filtered. The residue retained on the filter paper was oven-dried at 50 ° C overnight. The dried sample was ultrasonicated using a 12 mm probe at 20 kHz frequency in distilled water for 2 h. The suspension was lyophilized for further analysis.

Preparation of PLA/ANP films

PLA films reinforced with almond shell nanoparticles were prepared using the solvent casting method. ANP was sonicated in 20 mL of DCM for 10 min. The PLA, Tween80 and a suitable plasticizer were added to DCM and a casting solution was prepared under magnetic stirring at room temperature. In the case of PLA/ANP films, sonicated ANP solution was added to the PLA solution in various loadings (0.25, 0.5, 0.75 and 1% by wt) and kept under constant stirring for 4 h. Next, the solutions were cast into glass Petri plates and dried at room temperature overnight. The Petri dishes were stored at 25° C at 50% RH for 2 days prior to analysis.

Characterization of nanoparticles

Fourier-transform infrared spectroscopy (FTIR)

FTIR spectra for the untreated almond shell sample and the ball-milled sample were determined using an FTIR 6300 instrument (Jasco, Japan) with 0.07 cm^{-1} resolution over 4000–800 cm^{-1} range.

Particle size distribution

The particle size distributions of the dried ball-milled sample and the ultrasonicated sample were measured using an LA-950 type laser scattering particle size distribution analyzer (Horiba, Japan). In this method, the particle size was estimated by determining the intensity and the angle of the diffracted and scattered light by irradiating the sample with the laser light and converting the data into particle size distribution.

Scanning electron microscopy (SEM)

Morphological characterization of almond shell nanoparticles was carried out using SEM TESCAN Vega 3 SBU model. ANPs were sputter-coated with a thin layer of gold before microscopic observations. The SEM images were taken at an accelerating voltage of 10 kV at various magnifications.

Characterization of film property

The physical properties of the above film casting solutions were studied to determine their density and viscosity.

Mechanical properties

The tensile property of films was estimated using a universal tensile tester (International Equipments, Mumbai, India) as per ASTM D882. Rectangular-shaped specimens of sample having a width of 25 mm were tested at a crosshead speed of 50 mm/min with a gauge length of 100 mm [31]. The thickness of films was measured at five different points on each film surface using a thickness gauge and the average was taken.

Optical properties

Film transparency was observed using a spectrophotometer at 560 nm according to ASTM D1746 [29].

Water solubility (WS)

Film samples (each 2×2 cm^2) were cut and dried in an oven at 105 °C for 24 h, and were weighed (W_1). Then, the films were stirred in 15 mL distilled water at room temperature (25–28 ºC) for 24 h. Later, the samples were filtered through Whatman No.1 filter papers. The insolubilized fraction was dried at 105 °C for 24 h, and weighed (W_2) [32]. The WS of the films was determined using the following equation (1):

$$\mathrm{WS}\ (\%) = 100\left(W_1 - W_2\right)/W_1. \quad (1)$$

Water vapor permeability (WVP)

WVP is a vital factor in designing a food packaging material as water can result in microbial growth and deteriorative reaction [15]. WVP tests were performed as per ASTM (1996) method E96. The film was wrapped over a permeation cell of circular opening 0.000201 m^2. The cell was stored at 25 °C and 75% RH was maintained in the humidity chamber. Anhydrous calcium chloride (0% RH) was placed inside the cell [33]. After the permeation tests, the film thickness was measured and WVP (g pa^{-1} s^{-1} m^{-1}) was calculated as given in equation (2):

$$\mathrm{WVP} = \mathrm{WVTR} \times d/S\left(R_1 - R_2\right). \quad (2)$$

WVTR is the water vapor transmission rate, d is the film thickness, S is the saturation vapor pressure of water (Pa) at testing temperature (25 ºC), R: is the RH in the humidity control chamber, R_2 is the RH in the permeation cell.

Thermal stability

Thermogravimetric analysis (TGA) was carried out on TGA Q50-USA model in a nitrogen atmosphere. 5 mg of film sample was heated from room temperature to 700 °C at a rate of 20 °C/min under a gas flow rate of 30 mL/min, and weight loss of the samples against temperature was recorded [30].

Biodegradability test

Soil burial degradation tests were carried out as described by [34]. The microflora naturally present in the soil was used for degrading the films. Film samples were cut into 2×10 cm^2. These samples were then placed in different plastic boxes of $80 \times 15 \times 10$ cm dimensions. These plastic boxes were filled with soil of pH nearly 6.7. The film samples were then buried in the soil at a depth of 8 cm from the surface of the soil. These plastic boxes containing the samples were stored at room temperature (28 ºC) to 35 ºC with controlled soil humidity (20% to 40%) by sprinkling with water at regular time intervals after an interval of 5 days; the films were again weighed after degradation. The weight loss (WL) of each film sample was obtained using the following formula (3):

$$\mathrm{WL}\ (\%) = 100\left(M_0 - M_1\right)/M_0, \tag{3}$$

where M_0 is the weight of dry film before degradation and M_1 is the weight of dry film after degradation. Weight loss was measured for a span of 30 days.

Statistical analysis

Experiments were carried out in triplicate and represented in the form of Mean ± S.D. Ordinary one-way ANOVA was used for statistical analysis followed by Duncan's post hoc test. The significant difference was estimated with a confidence interval of 95% ($p < 0.05$).

Results and discussion

Almond shells were dried, ground and sieved to uniform size. Almond shell nanoparticles were prepared by a mechanochemical approach, in which ball milling was carried out in dilute acid concentration with subsequent ultrasonication. This novel strategy eliminates the usage of concentrated acids for nanoparticle synthesis, thereby reducing the complexity of the process, minimizing the processing cost and preventing the degradation of cellulosic content in the almond shells. The obtained almond shell nanoparticles were weighed to estimate the product yield and a nanoparticle yield of 88.23% was obtained after the process. These nanoparticles were characterized and used in PLA film fabrication.

FTIR analysis

The infrared spectra of the untreated almond shell powder and ball-milled ultrasonicated ANP were analyzed and plotted within 4000–800 cm^{-1} range and represented as in Fig. 1. The wide-band in the range of 3348 cm^{-1} shows the presence of stretching vibrations of the hydroxyl (–OH) groups [35]. The peak at 1739 cm^{-1} attributes to the carbonyl (C=O) groups due to the presence of carbonyl aldehyde groups and acetyl esters of hemicellulose and lignin. In the case of the treated sample, the intensity of the peak at 1739 cm^{-1} representing the carbonyl (C=O) groups is largely reduced, which represents the removal of major lignin and hemicellulose content from the sample [36]. This

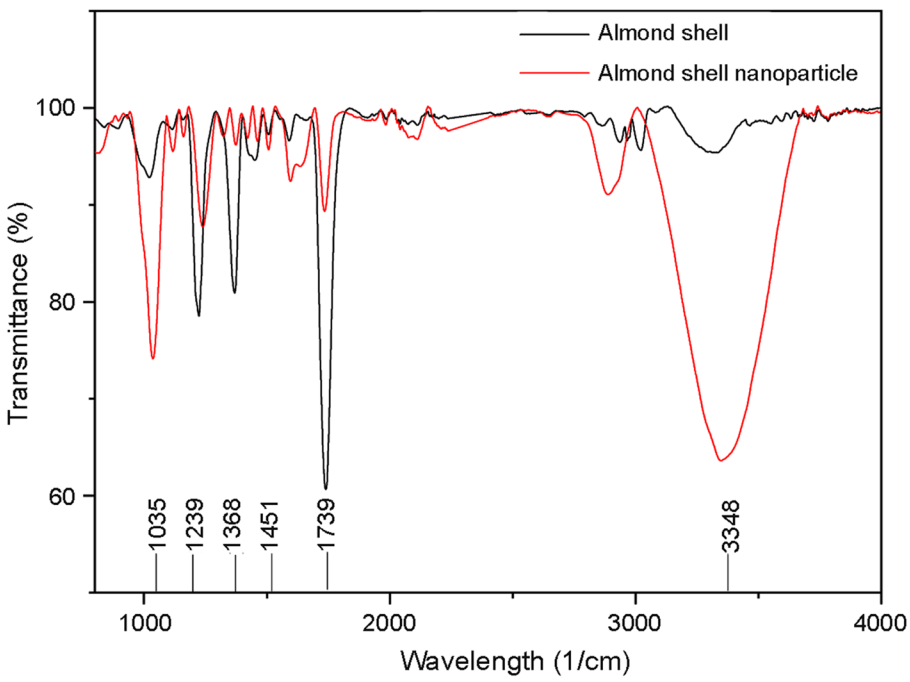

Fig. 1 FTIR spectrum of almond shell and almond shell nanoparticle

confirms that the mechanochemical approach has resulted in major removal of lignin and hemicellulose under dilute acid concentration, leaving only traces of lignin and hemicellulose in the treated sample. The absorption band at 1451 cm^{-1} has been reported for the asymmetric deformation vibration of the methyl group [37]. The peak at 1368 cm^{-1} represents the C–H bending. This peak is stronger in the untreated sample compared to the treated sample because of the C–CH_3 stretching present in the acetyl groups of hemicellulose, as it is reduced after the treatment [38]. Furthermore, the peak at 1239 cm^{-1} depicts the C–O stretching vibrations of the acyl group available in the lignin. This peak was reduced in the treated sample, which represents the removal of hemicellulose and lignin in the treated sample [39]. The band at 1035 cm^{-1} was found to be attributed to the C–O and C–C stretching of cellulose [40]. The FTIR spectral analysis confirms that a significant reduction in hemicellulose and lignin content is observed after ball milling and ultrasonication. Therefore, a major portion of amorphous molecules is removed after the treatment.

Table 1 Particle size distribution of treated almond shell

Particle size distribution for ball-milled sample	
Median size:	17.3 µm
Diameter on cumulative %	
D10:	10%–5.9 µm
D50:	50%–17.3 µm
D90:	90%–108.3 µm
Particle size distribution for ball-milled sample and ultrasonicated sample	
Median size:	197.2 nm
Diameter on Cumulative %	
D10:	10%–105 nm
D50:	50%–197 nm
D90:	90%–337 nm

Particle size distribution

The particle size distribution of almond shell particles after ball milling is tabulated in Table 1 and illustrated in Fig. 2. The mean size of almond shell particle after ball milling was determined to be 17.3 ± 4.5 µm. Mechanical disruption through ball milling has resulted in disintegration of almond shells to micro-sized particles. In this phenomenon, the almond shell particles undergo a strong high energy impact due to the prevailing collision between the alumina ball and the container wall. This collision of the particles that occurs in a dilute acid environment creates a number of microstructural alterations into the particles, leading to erosion of amorphous compounds. This progressive creation of collision results in crystallite size refinement [41]. In the next treatment, ultrasonication was performed to further refine the particles. The particles size of ball-milled and ultrasonicated sample represents that the average size of the particles reduced from 17.3 ± 4.5 µm to 197.2 ± 20.8 nm on intense ultrasonication. This shows that the size of the particles after ultrasonication reduced further down in comparison to that of the ball-milled sample. During ultrasonication, further erosion of amorphous compounds occurs due to the growth and collapse of microbubbles, creating shock waves in the dispersed particles thus largely contributing to the particle size reduction [42]. It was found that the size of the particles was greater than the nanoscale, which could be due to agglomeration of the particles in the sample due to the presence of strong hydrogen bonds [43].

Morphological analysis

The surface morphology of the almond shell powder and its structure after ball milling and ultrasonication treatments were studied using SEM as shown in Fig. 3. The almond shell powder prior to any treatments has a smooth, sheet-like structure as observed in Fig. 3a. This structure is broken

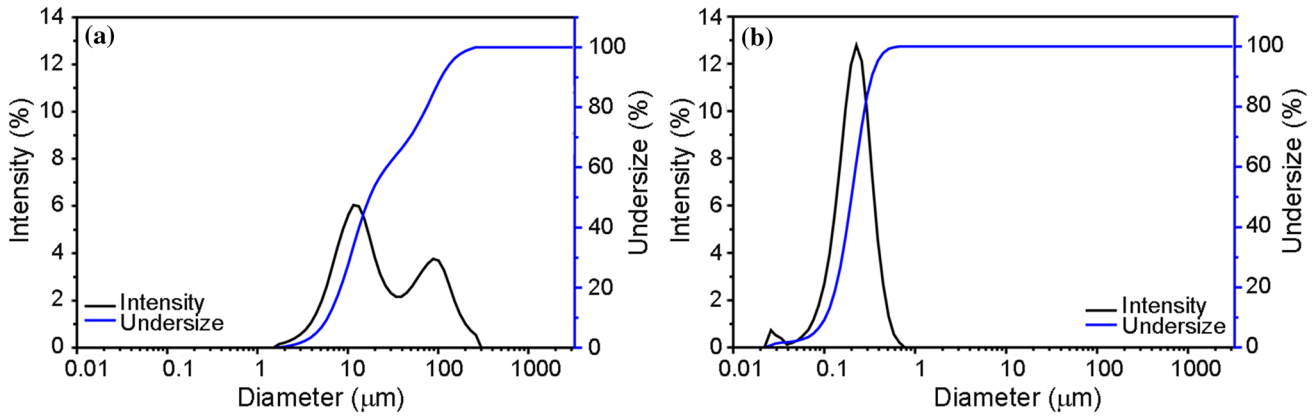

Fig. 2 Particle size distribution of **a** ball-milled sample and **b** ball-milled ultrasonicated almond shell nanoparticle

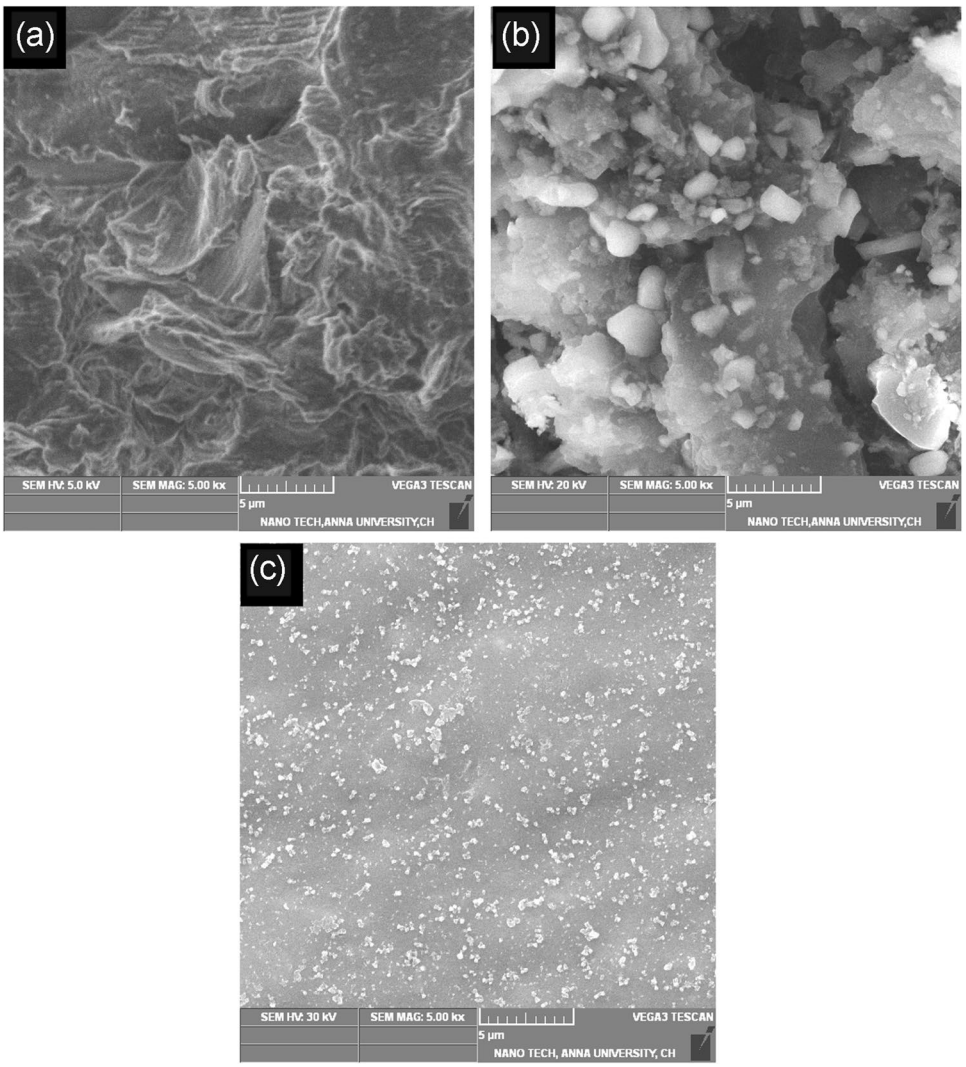

Fig. 3 Surface morphology of **a** almond shell powder, **b** ball-milled almond shell, and **c** ball-milled and ultrasonicated almond shell

down into separate microparticles by the ball milling process as shown in Fig. 3b. During the ball milling process, mechanical disruption is facilitated in a slightly acidic medium, which promotes the removal of the amorphous regions of the almond shell particle [44]. A wide distribution of particle size of the ball-milled sample can be observed with irregular sphere-like structures. The surface morphology of ANP after the ultrasonication process is illustrated in Fig. 3c. It can be observed that the almond shell particle size has reduced to a greater extent compared to the particle size after the ball milling by further removal of amorphous regions along the axial direction of the particle through ultrasonic cavitation [42].

Characterization of film property

The change in property of casting solution on addition of plasticizer was studied by measuring the density and viscosity of the casting solution (Table 2). Addition of plasticizer was found to decrease the viscosity of casting solution, thereby increasing its flexibility. The ANP particles obtained were reinforced in PLA film to enhance the mechanical and barrier property of the films. Since the incorporation of nanofillers tends to increase the rigidity of the films, a study on the plasticization of films was done prior to reinforcement to increase the elongation of the

Table 2 Properties of casting solution

Casting solution	Density (g/cm^3)	Viscosity (mPa s)
PLA	1.306	2.402
PLA + PEG (10%)	1.305	2.198
PLA + Glycerol (10%)	1.303	2.283
PLA + Sorbitol (10%)	1.296	2.185
PLA + Clove oil (10%)	1.301	2.009
PLA + Polycaprolactone (10%)	1.304	2.214

film. Fabricated films were further analyzed to test their biodegradability and thermal stability.

Mechanical properties

The study of the mechanical properties of PLA films is a subject of great concern due to their impact on product performance and consumer acceptance. Pure PLA is relatively rigid with higher tensile strength and more brittle with a lower percentage of elongation. The addition of plasticizer softens the film by reducing the intermolecular forces between the chains of PLA [15].

It is observed that the addition of plasticizers glycerol, sorbitol, clove oil, PEG and PCL at various concentrations of 2.5, 5.0, 7.5, 10.0, 12.5 and 15.0% (by w/w) had a significant impact on film property. Tensile strength significantly decreased on addition of plasticizer with probability value $p < 0.05$. A maximum tensile strength of 20.33 MPa was observed when PEG (12.5% by w/w) was used as plasticizer (Table 3). The OH groups present in PEG formed hydrogen bonding with PLA, which led to increased tensile strength. The addition of glycerol, sorbitol, clove oil and PCL significantly reduced the tensile strength to 16.32, 9.26, 12.3, 8.13 MPa, respectively. Elongation of the films significantly increased on addition of plasticizer ($p < 0.05$) and an exponential increase in elongation was observed as the concentration of plasticizer increased from 2.5 to 15.0%. Pure PLA films showed an elongation of 284.97%. The addition of PEG increased the elongation to 357.71%, and glycerol and sorbitol increased the elongation to 298.96% and 169.05%, respectively. The addition of polyols such as glycerol, sorbitol and PEG weakens the molecular interactions between the PLA polymers, and thus increases the free volume between the polymeric chains, enhancing the elongation of the developed films. PLA films showed a significant reduction in elongation (16.64%) on the addition of PCL as the plasticizer. The highest elongation-at-break (up to 377.19%) is seen when clove oil [10% (w/w)] is used, because it increases the free volume, eases the chain mobility of PLA and reduces the intermolecular forces between the PLA molecules. Among the other plasticizers, naturally derived clove oil has proven to significantly increase the elongation of the PLA films with only a slight decrease in tensile strength. Similar results have been confirmed in various researches using PLA and clove oil, where such films also exhibit strong antimicrobial and antioxidant properties, as reported in the literature [45, 46]. Further study was carried out using 10% clove oil as a plasticizer, which showed a higher elongation percentage with a minimum decrease in tensile strength of films compared to other plasticizers.

On the other hand, the addition of ANP to the PLA films significantly improved the tensile strength to 25.09 MPa ($p < 0.05$) as the nanoparticle loading increased up to 0.75% (Table 4), and similarly a slight decrease in elongation-at-break was observed as the concentration of ANP increased in the films. The elongation-at-break decreased from 377.19 to 368.24% due to the addition of ANP to the clove-plasticized PLA films. Higher reinforcement with nanoparticles creates a higher contact surface between ANP and PLA, thereby increasing the hydrogen bonding and Van der Waals bond of the molecules in the polymeric film and strengthening the molecular forces between them [47]. The amount of one percent of ANP was found to reduce tensile strength because excess particle distribution results in agglomeration and cluster formation of similar nanoparticles, thus disrupting the PLA matrix.

Optical properties

Transparency (TR) of a film is an important factor when it is applied for food packaging. The films obtained in this study were homogenous and transparent. From the result observed in Table 3, the transparency of films significantly reduced from 85.2% (pure PLA) to 67%, 65%, 64% and 55.2% with the addition of PEG, glycerol, sorbitol and PCL plasticizers, respectively. Clove oil (2.5% by w/w) showed the highest transparency (78%) than other plasticizers incorporated into the PLA films. A similar observation was reported by [48]. As the concentration of plasticizer increases, there is a drop in transparency, due to the crystal formation in PLA and also due to the increase in oil droplets in the clove oil-plasticized PLA matrix that interrupts the light passage. The addition of 1% ANP was also seen to decrease the film transparency significantly ($p < 0.05$) to 66.4%, because transparency is affected by the arrangement of amorphous and crystalline polymeric units, which are often seen in natural polymers like cellulose that is largely present in ANP [49]. These translucent packaging materials can be used for packing light-sensitive products [30, 45].

Water solubility

Water solubility of films is an important factor when it comes to packing of food products. Minimum water solubility is essential for food storage as it might affect the shelf life of foods. It is well known that PLA is insoluble in water. From the results observed in Table 2, 15% (by w/w) clove oil showed a minimum water solubility of 3.2%, whereas the addition of other plasticizers significantly increased the water solubility ($p < 0.05$). Maximum solubility of 22.2% was observed with the addition of 15% PEG. Addition of glycerol, sorbitol, PCL also increased the water solubility by14.5%, 14.1% and 18.6%, respectively, due to the presence of hydrophilic groups in the plasticizers [50]. Compared to the other plasticizers, films prepared using clove oil shows reduced water solubility of 3.2% due to an increase

Table 3 Effect of plasticizers on PLA-based films

Film composition	Average thickness (mm)	Tensile strength (MPa)	Elongation-at-break (%)	Optical property (%)	Water solubility (%)	Water vapor permeability $\times 10^{-10}$ (g Pa^{-1} s^{-1} m^{-1})	Biodegradation test (%)
PLA	0.091	20.34 ± 4.22	284.97 ± 42.41	85.2 ± 12.5	7.2 ± 1.5	2.29 ± 0.33	15.0 ± 1.7
PLA/PEG 2.5%	0.086	13.65 ± 2.12	128.87 ± 23.21****	77.4 ± 11.2	13.4 ± 2.2	1.44 ± 0.13	15.8 ± 0.7
PLA/PEG 5.0%	0.088	14.46 ± 3.24	176.81 ± 31.01*	75.0 ± 11.3	14.9 ± 2.2	1.41 ± 0.32	16.9 ± 1.2
PLA/PEG 7.5%	0.087	15.30 ± 3.33	296.41 ± 42.91	73.5 ± 11.7	16.6 ± 3.5*	1.36 ± 0.21	18.2 ± 2.7
PLA/PEG 10.0%	0.085	16.44 ± 2.11	316.55 ± 52.21	71.0 ± 12.1	19.7 ± 3.4***	1.33 ± 0.42	20.0 ± 1.1
PLA/PEG 12.5%	0.085	20.33 ± 5.16	357.23 ± 52.82	69.8 ± 9.2	21.1 ± 4.3****	1.30 ± 0.64	22.5 ± 2.4**
PLA/PEG 15.0%	0.086	20.08 ± 5.24	357.71 ± 52.30	67.0 ± 11.3	22.2 ± 4.8****	1.29 ± 0.64	24.0 ± 1.5***
PLA/Glycerol 2.5%	0.088	6.31 ± 1.62***	161.55 ± 23.24**	76.0 ± 12.9	9.1 ± 1.2	1.73 ± 0.03	12.5 ± 2.2
PLA/Glycerol 5.0%	0.089	12.79 ± 3.38	242.84 ± 31.54	73.8 ± 9.3	10.7 ± 3.1	1.41 ± 0.56	13.3 ± 1.6
PLA/Glycerol 7.5%	0.086	12.91 ± 2.41	250.15 ± 32.66	71.5 ± 8.6	11.2 ± 2.9	1.23 ± 0.13	14.2 ± 3.1
PLA/Glycerol 10.0%	0.085	13.43 ± 3.22	272.16 ± 31.33	69.3 ± 7.3	12.4 ± 3.5	1.18 ± 0.63	15.0 ± 2.0
PLA/Glycerol 12.5%	0.085	14.05 ± 4.35	287.31 ± 42.31	67.0 ± 12.3	13.4 ± 3.2	0.96 ± 0.03**	18.7 ± 1.0
PLA/Glycerol 15.0%	0.090	16.32 ± 4.42	298.96 ± 42.66*	65.0 ± 10.2	14.5 ± 4.5	0.88 ± 0.07**	20.0 ± 1.1
PLA/Sorbitol 2.5%	0.090	9.20 ± 1.66*	189.02 ± 21.88	74.0 ± 11.8	5.6 ± 1.6	0.89 ± 0.13**	12.9 ± 1.9
PLA/Sorbitol 5.0%	0.088	10.10 ± 2.71	219.54 ± 32.43	72.5 ± 9.9	7.4 ± 2.8	1.46 ± 0.26	14.7 ± 1.4
PLA/Sorbitol 7.5%	0.087	12.64 ± 3.61	228.07 ± 33.29	70.1 ± 10.1	11.8 ± 2.3	1.50 ± 0.33	16.2 ± 2.6
PLA/Sorbitol 10.0%	0.088	14.24 ± 3.26	240.38 ± 34.22	68.0 ± 8.2	12.1 ± 2.9	1.64 ± 0.53	17.0 ± 1.5
PLA/Sorbitol 12.5%	0.086	15.89 ± 4.88	281.31 ± 42.75	66.2 ± 6.6	13.2 ± 2.3	1.85 ± 0.26	19.3 ± 2.5
PLA/Sorbitol 15.0%	0.085	9.26 ± 2.21*	169.05 ± 21.33	64.0 ± 9.4	14.1 ± 2.2	2.04 ± 0.32	21.0 ± 3.0
PLA/Clove Oil 2.5%	0.088	11.36 ± 3.06	193.82 ± 22.99	78.0 ± 7.3	8.6 ± 1.7	1.53 ± 0.14	15.2 ± 1.3
PLA/Clove Oil 5.0%	0.089	13.96 ± 2.35	230.80 ± 23.28	77.2 ± 8.7	7.4 ± 1.6	1.39 ± 0.31	16.3 ± 1.8
PLA/Clove Oil 7.5%	0.091	19.69 ± 4.83	332.32 ± 30.41	75.9 ± 6.9	6.3 ± 1.4	1.17 ± 0.15	17.5 ± 1.2
PLA/Clove Oil 10.0%	0.089	19.75 ± 4.91	377.19 ± 43.21	75.0 ± 5.2	5.7 ± 1.5	0.87 ± 0.13**	18.0 ± 1.1
PLA/Clove Oil 12.5%	0.088	18.14 ± 4.22	328.57 ± 32.32	74.1 ± 9.2	4.8 ± 1.1	0.68 ± 0.15***	22.1 ± 2.5*
PLA/Clove Oil 15.0%	0.087	12.30 ± 2.31	306.62 ± 32.44	72.0 ± 8.1	3.2 ± 0.9	0.74 ± 0.19***	23.0 ± 2.4**
PLA/PCL 2.5%	0.088	5.82 ± 1.16***	16.64 ± 2.41****	75.0 ± 9.1	10.1 ± 2.5	1.41 ± 0.28	16.2 ± 2.2
PLA/PCL 5.0%	0.088	6.13 ± 1.18***	18.21 ± 5.45****	74.2 ± 7.1	12.2 ± 2.8	1.32 ± 0.23	17.0 ± 1.7
PLA/PCL 7.5%	0.084	8.22 ± 2.12***	20.17 ± 4.41****	65.3 ± 7.7	13.2 ± 3.5	1.31 ± 0.22	18.7 ± 1.4
PLA/PCL 10.0%	0.085	9.17 ± 2.15**	23.39 ± 7.51****	59.7 ± 6.1	15.2 ± 2.5	1.30 ± 0.66	20.0 ± 2.7

Table 3 (continued)

Film composition	Average thickness (mm)	Tensile strength (MPa)	Elongation-at-break (%)	Optical property (%)	Water solubility (%)	Water vapor permeability $\times 10^{-10}$ (g Pa^{-1} s^{-1} m^{-1})	Biodegradation test (%)
PLA/PCL 12.5%	0.084	8.91 ± 2.52*	21.17 ± 6.11****	57.3 ± 8.9	16.5 ± 4.2*	1.29 ± 0.46	22.8 ± 2.1**
PLA/PCL 15.0%	0.083	8.13 ± 1.53**	22.26 ± 5.01****	55.2 ± 6.9	18.6 ± 4.5**	1.27 ± 0.31	24.0 ± 1.7***

Results are represented as Mean ± S.D

*Represents significant differences between values ($P < 0.05$)

**Represents significant differences between values ($P < 0.01$)

***Represents significant differences between values ($P < 0.001$)

****Represents significant differences between values ($P < 0.0001$)

Table 4 Effect of almond shell nanoparticle addition on PLA-based films

Sample	Average thickness (mm)	Tensile strength (MPa)	Elongation-at-break (%)	Optical property (%)	Water solubility (%)	Water vapor permeability $\times 10^{-10}$ (g Pa^{-1} s^{-1} m^{-1})	Biodegradation test (%)
PLA/Clove oil (10%)	0.089	19.75 ± 2.91	377.19 ± 33.21	75.0 ± 2.0	5.7 ± 0.5	0.87 ± 0.13	18.0 ± 1.1
PLA/Clove oil (10%) /ANP (0.25%)	0.088	20.21 ± 4.22	374.80 ± 42.81	74.0 ± 2.1	8.7 ± 0.3***	0.33 ± 0.07**	18.2 ± 1.5
PLA/Cloveoil (10%)/ANP (0.5%)	0.086	23.28 ± 4.22****	372.79 ± 31.31	69.2 ± 1.2*	9.2 ± 0.9***	0.31 ± 0.09**	20.5 ± 2.7
PLA/Clove oil (10%)/ANP (0.75%)	0.090	25.09 ± 3.22****	370.98 ± 42.91	68.0 ± 1.4**	10.5 ± 1.6****	0.30 ± 0.13**	21.4 ± 2.6
PLA/Clove oil (10%)/ANP (1.0%)	0.091	23.88 ± 4.22****	368.24 ± 42.13*	66.4 ± 1.9***	10.5 ± 1.2****	0.25 ± 0.15***	23.2 ± 0.7*

Results are represented as Mean ± S.D

*Represents significant differences between values ($P < 0.05$)

**Represents significant differences between values ($P < 0.01$)

***Represents significant differences between values ($P < 0.001$)

****Represents significant differences between values ($P < 0.0001$)

in hydrophobicity of the PLA films due to the addition of clove oil. Addition of ANP has resulted in a slight increase in solubility to 10.5% due to disorganization of the crystalline structure during processing, but compared to the other biopolymeric films reported in the literature [50, 51], the developed PLA films showed its minimum water solubility that can be used for food products packing.

Water vapor permeability

Water vapor permeability (WVP) of a film is an important property that greatly controls the utility of film for packing of different types of foods. WVP tests were carried out for PLA films with various concentrations of plasticizer. It showed that in Table 3, the addition of plasticizer gradually decreases the WVP compared to pure PLA with WVP of 2.29×10^{-10} gPa^{-1} s^{-1} m^{-1}. The addition of 15% PEG, glycerol and PCL showed a decrease in WVP to 1.29×10^{-10}, 0.88×10^{-10} and 1.27×10^{-10} gPa^{-1} s^{-1} m^{-1}, respectively. A significant reduction in WVP to 0.87×10^{-10} gPa^{-1} s^{-1} m^{-1} was observed when a higher concentration of clove oil was used. Clove oil which is hydrophobic in nature restricts the transfer of water vapor through the film and thereby decreases the WVP.

Similarly, the addition of ANP (1%) has been found to significantly reduce the water vapor permeability to

0.25×10^{-10} gPa^{-1} s^{-1} m^{-1} due to the creation of a network of hydrogen bridges between the polymer and the nanoparticles, producing a tortuous path to the water vapor passing through the film [47].

Thermal stability

The thermal stability of the plasticized PLA films at a plasticizer concentration of 10% and ANP/PLA films was examined by TGA. The weight loss versus temperature curves are shown in Fig. 4. The plasticized PLA films and ANP/PLA were degraded about 100% with respect to their initial weight during heating between 300 and 380 °C. Thermal degradation of about 5% of the PLA films was determined at 260 °C for sorbitol-plasticized films and at 270 °C for the other plasticized films. Degradation of 5% was found earlier at a temperature of 250 °C for ANP/PLA films, which might be due to the degradation of ANP. It can also be seen that 50% weight loss has occurred at 370 °C for PCL-plasticized PLA and at 350 °C for the other plasticized films and at 310 °C for ANP/PLA films. The maximum degradation was found to be at 470 °C for PCL-plasticized PLA whereas for others it was relatively at a lesser temperature as shown in Table 5. The thermal degradation at $T_{5\%}$ and $T_{max\%}$ of clove oil-plasticized PLA and pure PLA is the same, which signifies that the thermal stability of PLA was not affected after the addition of plasticizer. But the addition of ANP showed degradation at a temperature slightly below 250 °C. The temperature range of 250–350 °C indicates the degradation of PLA, and similar findings were also reported by [9, 52]. TGA results signify that the addition of plasticizer and nanoparticle did not decrease the thermal stability of the PLA films largely, and thus, they are suitable to be used in the extrusion process for large-scale production.

Biodegradability test

Weight loss of films during soil burial test can be taken as an indicator of biodegradation. The weight loss is a reflection of the biodegradation process by the moisture and micro-organism of the soil. PLA films showed significant degradation and loss of transparency after 5 days. The

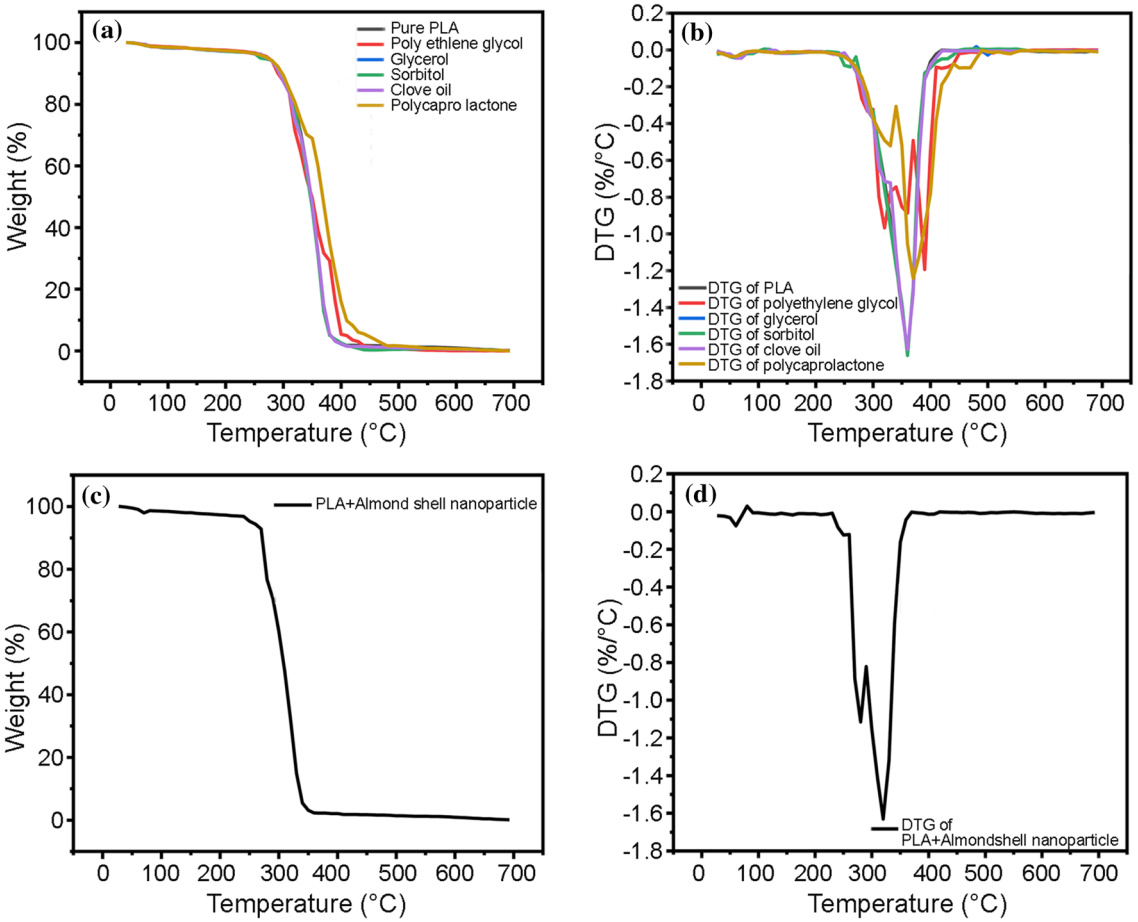

Fig. 4 TGA of **a** plasticized PLA, **b** DTG of plasticized PLA, **c** TGA of ANP/PLA film, and d DTG of ANP/PLA film

Table 5 Thermal stability of PLA films

	Samples	$T_{5\%}$ (°C)	$T_{50\%}$ (°C)	T_{max}%(°C)
1	Pure PLA	270	350	410
2	PLA + 10% Polyethylene glycol	270	350	430
3	PLA + 10% Glycerol	270	350	410
4	PLA + 10% Sorbitol	260	350	420
5	PLA + 10% Clove Oil	270	350	410
6	PLA + 10% Polycaprolactone	270	370	470
7	PLA + 10% Clove Oil + 0.75% ANP	250	310	410

results of the soil burial degradation test showed that pure PLA films were degraded to max 15%, plasticized-PLA films were degraded to max 24% and PLA/ANF films were degraded by 23.2% in a span of 30 days (Tables 2 and 3). Complete degradation of the films was seen in a span of 6 months.

Conclusion

In the current study, almond shell nanoparticles were prepared by a mechanochemical process and were used as nanofillers in PLA films. Various concentrations of plasticizers (2.5 to 15% by wt of PLA) have been used to improve the mechanical properties of PLA. The synergistic effect of plasticizer and ANP in PLA films was analyzed. PLA blend involving 10% (w/w) clove oil increased the elongation-at-break by 377.19%, and tensile strength, with the addition of 0.75% ANF, was increased by 25.09 N/mm^2. Pure PLA films showed a higher transparency by 85.2% compared to PLA plasticized with 2.5% (w/w) clove oil (by 78%) and nanoparticle reinforced films. Water solubility of pure PLA was 7%, whereas the addition of plasticizer (15% by w/w clove oil) it was reduced to 3%, but the addition of nanoparticles increased the solubility of films to 10.5%. WVP of pure PLA film was 2.2980×10^{-10} g Pa^{-1} s^{-1} m^{-1}, and the addition of 1% ANF significantly reduced the WVP to 0.25×10^{-10} g Pa^{-1} s^{-1} m^{-1}. Thermogravimetric analysis of the PLA films proved that the films were thermally stable at 250 °C. Soil burial degradation test confirmed complete degradation of PLA films in a span of 6 months. In conclusion, the insights obtained from this study have suggested that the PLA/clove oil/ANP-based as packaging films can be a better alternative packaging material owing to their enhanced mechanical and barrier property.

Data availability All data generated or analyzed during this study are included in this published article.

Declarations

Conflict of interest The authors have no conflicts of interest to declare that are relevant to the content of this article.

References

1. Ibanez-Garcia A, Martinez-Garcia A, Ferrandiz-Bou S (2021) Influence of almond shell content and particle size on mechanical properties of starch based biocomposites. Waste Biomass Valori 2:5823–5836
2. Khosravi A, Fereidoon A, Mehdi M, Naderi G (2020) Soft and hard sections from cellulose-reinforced poly (lactic acid) -based food packaging films: A critical review. Food Packag Shelf Life 23:100429
3. Kamaludin NHI, Ismail H, Rusli A, Ting SS (2021) Thermal behavior and water absorption kinetics of polylactic acid/ chitosan biocomposites. Iran Polym J 30:135–147
4. Casagrande M, Zanela J, Wagner Junior A, Yamashita F, Busso C, Wouk J, Radaelli JC, Malfatti CRM (2021) Optical, mechanical, antioxidant and antimicrobial properties of starch/ polyvinyl alcohol biodegradable film incorporated with Bacharisdracunculifolia lyophilized extract. Waste Biomass Valori 12:3829–3848
5. Yu L, Dean K, Li L (2006) Polymer blends and composites from renewable resources. Prog Polym Sci 31:576–602
6. Zhu YQ, Romain C, Williams CK (2016) Sustainable polymers from renewable resources. Nature 540:354–362
7. Liu Z, Hu D, Huang L (2018) Simultaneous improvement in toughness, strength and biocompatibility of poly(lactic acid) with polyhedral oligomeric silsesquioxane. Chem Eng J 346:649–661
8. He JF, Lv XG, Lin QB, Li Z, Liao J, Xu CY, Zhong WJ (2019) Migration of metal elements from polylactic acid dinner plate into acidic food simulant and its safety evaluation. Food Packag Shelf Life 22:100381
9. Risyon NP, Othman SH, Basha RK, Talib RA (2020) Characterization of polylactic acid/halloysite nanotubes bionanocomposite films for food packaging. Food Packag Shelf Life 23:100450
10. Arjmandi R, Hassan A, Haafiz MKM, Zakaria Z (2015) Partial replacement effect of montmorillonite with cellulose nanowhiskers on polylactic acid nanocomposites. Int J Biol Macromol 81:91–99
11. Hapuarachchi TD, Peijs T (2010) Multiwalled carbon nanotubes and sepiolitenanoclays as flame retardants for polylactide and its natural fibre reinforced composites. Compos A 41:954–963
12. Sanusi OM, Benelfellah A, Bikiaris DN, AitHocine N (2020) Effect of rigid nanoparticles and preparation techniques on the performances of poly(lactic acid) nanocomposites: A review. Polym Adv Technol 32:444–460
13. Raisipour-Shirazi A, Ahmadi Z, Garmabi H (2018) Polylactic acid nanocomposites toughened with nanofibrillated cellulose: microstructure, thermal, and mechanical properties. Iran Polym J 27:785–794
14. EnumoJr A, Gross IP, Saatkamp RH, Pires ATN, Parize AL (2020) Evaluation of mechanical, thermal and morphological properties of PLA films plasticized with maleic acid and its propyl ester derivatives. Polym Test 88:106552
15. Bhasney SM, Patwa R, Kumar A, Katiyar V (2017) Plasticizing effect of coconut oil on morphological, mechanical, thermal, rheological, barrier, and optical properties of poly(lactic acid): A promising candidate for food packaging. J Appl Polym Sci 134:45390

16. Boudjema HL, Bendaikha H, Maschke U (2020) Green composites based on Atriplexhalimus fibers and PLA matrix. J Polym Eng 40:693–702
17. Xi X, Zhen W, Bian S (2015) Preparation and properties of polylactic acid /*N*-(2-hydroxyl) propyl-3-trimethyl ammonium chloride-intercalated saponite nanocomposites. Iran Polym J 24:243–252
18. Garcia AM, Garcia AI, Cabezas MAL, Reche AS (2015) Study of the influence of the almond variety in the properties of injected parts with biodegradable almond shell based master batches. Waste Biomass Valori 6:363–370
19. Marquis DM, Guillaume E, Chivas-Joly C (2011)Properties of nanofillers in polymer, nanocomposites and polymers with analytical methods. John Cuppoletti, Intech Open
20. Garzon E, ArceC C-F, Perez-Falcon JM, Sanchez-Soto PJ (2021) Thermal behavior of the different parts of almond shells as waste biomass. J Therm Anal Calorim 147:5023–5035
21. Xuemin L, Yinan L, Jianxiu H, Weihong W (2018) Study of almond shell characteristics Materials 11:1782
22. Shrestha S, Kognou ALM, Zhang J, Qin W (2021) Different facets of lignocellulosic biomass including pectin and its perspectives. Waste Biomass Valori 12:4805–4823
23. Toles CA, Marshall WE, Johns MM, Wartelle LH, McAloon A (2000) Acid activated carbons from almond shells: physical, chemical and adsorptive properties and estimated cost of production. Bioresour Technol 71:87–92
24. Senturk HB, Ozdes D, Duran C (2010) Biosorption of Rhodamine 6G from aqueous solutions onto almond shell (Prunusdulcis) as a low cost biosorbent. Desalination 252:81–87
25. Mohan D, Sarswat A, Singh VK, Alexandre-Franco M, Pittman CU (2011) Development of magnetic activated carbon from almond shells for trinitrophenol removal from water. Chem Eng J 172:1111–1125
26. Essabir H, Nekhlaoui S, Malha M, Bensalah MO, Arrakhi FZ, Qaiss A, Bouhfid R (2013) Bio-composites based on polypropylene reinforced with almond shell particles: mechanical and thermal properties. Mater Des 51:225–230
27. Chaudhary AK, Gope PC, Singh VK (2015) Water absorption and thickens swelling behavior of almond *(Prunusamygdalus L)* shell particles and coconut *(Cocos nucifera)* fiber hybrid epoxy-based biocomposite. Sci Eng Compos Mater 22:375–382
28. Altay L, Guven A, Atagur M, Uysalman T, Tantug GS, Ozkaya M, Sever K (2019) Linear low density polyethylene filled with almond shells particles: mechanical and Thermal Properties. Acta Phys Pol, A 2019:135
29. El Mechtali FZ, Essabir H, Nekhlaoui S, Bensalah MO, Jawaid M, Bouhfid R, Qaiss A (2015) Mechanical and thermal properties of polypropylene reinforced with almond shells particles: impact of chemical treatments. J Bionic Eng 12:483–494
30. Sharma S, Singh AA, Majumdar A, Butola BS (2019) Tailoring the mechanical and thermal properties of polylactic acid-based bionanocomposite films using halloysite nanotubes and polyethylene glycol by solvent casting process. J Mater Sci 54:8971–8983
31. Ulloa PA, Vidal J, Dicastillo CL, de Rodriguez F, Guarda A, Cruz RMS, Galotto MJ (2018) Development of poly(lactic acid) films with propolis as a soure of active compounds: biodegradability, physical and functional properties. J Appl Polym Sci 136:47090
32. Wu J, Liu H, Ge S, Wan S, Qin Z, Chen L, Zhang Q (2015) The preparation, characterization, antimicrobial stability and invitro release evaluation of fish gelatin films incorporated with cinnamon essential oil nanoliposomes. Food Hydrocoll 43:427–435
33. Mali S, Grossmann MVE, García MA, Martino MN, Zaritzky NE (2004) Barrier, mechanical and optical properties of plasticized yam starch films. Carbohydr Polym 56:129–135
34. Maran JP, Sivakumar V, Thirugnanasambandham K, Sridhar R (2014) Degradation behavior of biocomposites based on cassava starch buried under indoor soil conditions. Carbohydr Polym 101:20–28
35. Gea S, Indra Muis Y, Nami P, Yasir AH (2019) Preparation of polyvinyl alcohol/cellulose nanofiber nanocomposite isolated from empty oil palm fruit bunches. IOP Conference Series: Mater Sci Eng 553:012041
36. Lu Q, Tang L, Wang S, Huang B, Chen Y, Chen X (2014) An investigation on the characteristics of cellulose nanocrystals from Pennisetumsinese. Biomass Bioenerg 70:267–272
37. Smith RC (1961) Infrared spectra of substituted 1,10-phenanthrolines. Retrospective Theses and Dissertations, Iowa State University
38. Ma Q, Mohawk D, Jahani B, Wang X, Chen Y, Mahoney A, Zhu JY, Jiang L (2020) UV-Curable cellulose nanofiber-reinforced soy protein resins for 3D printing and conventional moulding. ACS Appl Polym Mater 2:4666
39. Ambone T, Torris A, Shanmuganathan K (2020) Enhancing the mechanical properties of 3D printed polylactic acid using nanocellulose. Polym EngSci60:1842–1855
40. Li W, Cai G, Zhang P (2019) A simple and rapid Fourier transform infrared method for the determination of the degree of acetyl substitution of cellulose nanocrystals. J Mater Sci 54:8047–8056
41. Amirkhanlou S, Ketabchi M, Parvin N (2012) Nanocrystalline/nanoparticle ZnO synthesized by high energy ball milling process. Mater Lett 86:122–124
42. Yadav C, Saini A, Maji PK (2017) Energy efficient facile extraction process of cellulose nanofibres and their dimensional characterization using light scattering techniques. Carbohydr Polym 165:276–284
43. Di Giorgio L, Martín L, Salgado PR, Mauri AN (2020) Synthesis and conservation of cellulose nanocrystals. Carbohydr Polym 238:116187
44. Nuruddin M, Hosur M, Uddin MJ, Baah D, Jeelani S (2016) A novel approach forextracting cellulose nanofibers from lignocellulosic biomass by ball milling combined withchemical treatment. J Appl Polym Sci 133:42990
45. Arfat YA, Ahmed J, Ejaz M, Mullah M (2017) Polylactide/graphene oxide nanosheets/clove essential oil composite films for potential food packaging applications. Int J Biol Macromol 107:194–203
46. Qin Y, Li W, Liu D, Yuan M, Li L (2017) Development of active packaging film made from poly(lactic acid) incorporated essential oil. Prog Org Coat 103:76–82
47. Aila-Suarez S, Palma-Rodriquez HM, Rodriguez-Hernandez AI, LA Hernandez-UribeJP B-P, Vargas-Torres A (2013) Characterization of films made with chayote tuber and potato starches blending with cellulose nanoparticles. Carbohydr Polym 98:102–107
48. Miao L, Walton WC, Wang L, Li L, Wang Y (2019) Characterization of polylactic acids-polyhydroxybutyrate based packaging film with fennel oil and its application on oysters. Food Packag Shelf Life 22:100388
49. Acharya S, Hu Y, Moussa H, Abidi N (2017) Preparation and characterization of transparent cellulose films using an improved cellulose dissolution process. J Appl Polym Sci 134:44871
50. Ulfah M, Salsabila A, Rohmawati I (2017) Characterisitics of water solubility and color on edible film from bioselulosanatanirasiwalan with the additional of glycerol. J Phys 983:012191
51. Slavutsky AM, Bertuzzi MA (2014) Water barrier properties of starch films reinforced with cellulose nanocrystals obtained from sugarcane bagasse. Carbohydr Polym 110:53–61
52. Al-Itry R, Lamnawar K, Maazouz A (2012) Improvement of thermal stability, rheological and mechanical properties of PLA, PBAT and their blends by reactive extrusion with functionalized epoxy. Polym Degrad Stabil 97:1898–1914